

# Electrical conductivity enhanced dielectric and piezoelectric properties of ferroelectric 0-3 composites

C. K. Wong<sup>a)</sup>

*Department of Applied Physics, The Hong Kong Polytechnic University, Hong Kong, China*

F. G. Shin

*Department of Applied Physics, Materials Research Center and Center for Smart Materials, The Hong Kong Polytechnic University, Hong Kong, China*

(Received 8 September 2004; accepted 29 December 2004; published online 14 March 2005)

We have investigated the effects of electrical conductivity of the constituents on the dielectric and piezoelectric properties of ferroelectric 0-3 composites. The time-dependent internal electric fields are first derived, which can be induced by an applied ac field in dielectric measurement or stress in piezoelectric measurement. Our previously developed model [C. K. Wong, Y. M. Poon, and F. G. Shin, *J. Appl. Phys.* **90**, 4690 (2001)] has been extended to include the additional contribution from the electrical conductivities and the frequency of measurement, which can be significant for ceramic/polymer composites possessing high conductivity in the matrix phase. The model provides an explanation to the surprisingly high piezoelectric  $d_{33}$  values reported by, e.g., Chen *et al.* [*Sens. Actuators, A* **65**, 194 (1998)]. Explicit expressions for the transient and steady-state responses are given and the effective permittivity,  $d_{33}$ ,  $d_{31}$ , and  $d_h$  coefficients have been derived. © 2005 American Institute of Physics. [DOI: 10.1063/1.1862317]

## I. INTRODUCTION

One of the primary goals of embedding piezoelectric ceramic particles within a polymer matrix (i.e., 0-3 composite) is to combine the better properties of ceramic and polymer. Ferroelectric ceramics have high piezoelectric properties, but their poor mechanical properties and the large difference in acoustic impedance with water restrict their usage for certain applications. Ferroelectric polymers, on the other hand, have good mechanical flexibility, but their piezoelectric  $d$  values are low. The use of ferroelectric composites seems capable of overcoming these deficiencies and their properties can be tailored for specific applications. One may in principle design a 0-3 composite with high ceramic volume fraction for applications necessitating high piezoelectric  $d$  values. However, it is difficult to fabricate a 0-3 composite sample of high ceramic concentration and the high ceramic content will also lower the flexibility of the composite.

To improve the piezoelectric (as well as pyroelectric) properties of 0-3 composites and also for facilitating poling, Sakamoto *et al.* attempted to fabricate graphite doped lead zirconate titanate/polyurethane (PZT/PU) 0-3 composites.<sup>1</sup> By adding about 1% by volume of graphite to increase the electrical conductivity of PU, both the pyroelectric and piezoelectric  $d_{33}$  coefficients of the composite increased. Indeed, the effect of higher conductivity in the polymer matrix is not limited only to enhancing the pyroelectric and piezoelectric properties. Recently we find that, in the poling process of ferroelectric composites, it shortens the time development of the electric field acting on the ceramic to reach saturation, therefore, poling of the ceramic phase in such composite systems can be more efficient,<sup>2,3</sup> which is of prac-

tical significance since the pyroelectric and piezoelectric activities of the constituents are generally proportional to their degree of poling.<sup>3,4</sup>

In another report, Chen *et al.* investigated the influence of solvent treatment on the piezoelectric and dielectric properties of a ferroelectric 0-3 composite.<sup>5</sup> They immersed the composite sample of lead zirconate titanate/polyvinylidene fluoride (PZT/PVDF) in a certain solvent [e.g., *N*-dimethylacetamide (DMA)] for a period of time. The piezoelectric and dielectric properties were measured after the sample was removed from the solvent environment. They observed that both the permittivity and  $d_{33}$  coefficient were one to five times larger than those of the virgin specimen. Such high values are quite likely to be out of reach of the existing model predictions for “normal” dielectric and piezoelectric 0-3 composites. Chen *et al.* suggested that the polymer was swollen by the soaking solvent and the swollen composite would then “transform” from 0-3 to 1-3 type, hence the enhanced  $d_{33}$  value.<sup>5</sup> We believe that these enhancements could very well be related to the increment of electrical conductivity in the matrix material brought about by the solvent. Actually, the use of different solvent treatments with varying concentration has been a popular technique to increase the conductivity of polymer electrolytes, in which a considerable amount of research work has been done due to the potential application in solid-state batteries, etc.<sup>6–10</sup>

This work attempts to investigate the effect of electrical conductivity on the dielectric and piezoelectric properties of a ferroelectric composite of a dispersion of spherical inclusions in a continuous matrix, assuming the constituents possess finite conductivity. The sample is excited by an ac electric field (dielectric measurement) or ac stress (piezoelectric measurement) of small amplitude. An analytical model is

<sup>a)</sup>Electronic mail: wongck.a@polyu.edu.hk

proposed and explicit expressions are derived for the dynamic behavior of the electric fields in the constituents. The steady-state solutions are then used to obtain explicit expressions for the effective permittivity,  $d_{31}$ ,  $d_{33}$ , and  $d_h$  coefficients. Compared to the Maxwell–Wagner formula<sup>11</sup> for permittivity and our previously derived analytical expressions (for  $d_{31}$ ,  $d_{33}$ , and  $d_h$ ),<sup>12</sup> which assume perfectly insulating constituents, the set of expressions contains a factor describing the coupled effects of permittivity, conductivity, and the measuring frequency. Theoretical evaluations are based on the constituent parameters of PZT/PVDF. The surprisingly large  $d_{33}$  values reported by Chen *et al.* can be qualitatively simulated by assuming an increase in the conductivity of PVDF after soaking in solvent.<sup>5</sup> We will demonstrate that this enhancement will naturally be significant for samples with a mildly conductive matrix phase.

## II. THEORY

To find the effective permittivity and piezoelectric  $d$  coefficients of a 0-3 composite of two ferroelectric phases, we will first obtain the time development of the internal electric fields within the individual phases, given the external sinusoidal electric field and stress. Then the steady-state solution of the in-phase component of internal fields will be used to obtain expressions for the permittivity,  $d_{31}$ ,  $d_{33}$ , and  $d_h$  coefficients.

### A. A formulation for calculating the dynamic behavior of internal electric fields

Suppose the composite is initially polarized in the  $z$  direction, in which case we only need to be concerned with the electric field and polarization in the “3” direction. We first

write the volumetric average electric displacement  $D$  and conduction current density  $j$  for the ferroelectric constituent materials in the composite as<sup>13</sup>

$$\begin{cases} \langle D_{3i} \rangle = \varepsilon_i \langle E_{3i} \rangle + \langle P_{3i} \rangle \\ \langle D_{3m} \rangle = \varepsilon_m \langle E_{3m} \rangle + \langle P_{3m} \rangle, \end{cases} \quad (1)$$

$$\begin{cases} \langle j_{3i} \rangle = \sigma_i \langle E_{3i} \rangle \\ \langle j_{3m} \rangle = \sigma_m \langle E_{3m} \rangle, \end{cases} \quad (2)$$

where the angular brackets denote volume-averaged fields enclosed.  $P$  is polarization,  $\varepsilon$  and  $\sigma$  denote permittivity and electrical conductivity, respectively, and  $E$  is electric field. Subscripts  $i$  and  $m$  denote “inclusion” and “matrix,” respectively.

Consider the single inclusion problem of a ferroelectric sphere surrounded by a ferroelectric matrix medium with a uniform electric field applied along the  $z$  direction far away from the inclusion. The boundary-value problem gives the following equations:<sup>13</sup>

$$\langle D_{3i} \rangle + 2\varepsilon_m (\langle E_{3i} \rangle - \langle E_{3m} \rangle) = \langle D_{3m} \rangle - q_0, \quad (3)$$

$$\langle j_{3i} \rangle + 2\sigma_m (\langle E_{3i} \rangle - \langle E_{3m} \rangle) = \langle j_{3m} \rangle + \partial q_0 / \partial t. \quad (4)$$

In Eqs. (3) and (4), we have assumed that both constituent materials are uniformly polarized and the homogeneously polarized sphere is covered with surface charge of density  $q_0$  at the pole along the polarizing direction ( $\theta=0$ ) with a distribution given by  $q_0 \cos \theta$ .

For a composite comprising a dilute suspension of spherical particles uniformly distributed in the matrix material, the volumetric averages of the electric fields satisfy<sup>12</sup>

$$\langle E_3 \rangle = \phi \langle E_{3i} \rangle + (1 - \phi) \langle E_{3m} \rangle, \quad (5)$$

where  $\phi$  is the volume fraction of the inclusion phase. We obtain from Eqs. (1)–(5)

$$\frac{\partial \langle E_{3i} \rangle}{\partial t} + \frac{\langle E_{3i} \rangle}{\tau} = \frac{3[\sigma_m \langle E_3 \rangle + \varepsilon_m \partial \langle E_3 \rangle / \partial t] + (1 - \phi) \partial [\langle P_{3m} \rangle - \langle P_{3i} \rangle] / \partial t}{\phi 3\varepsilon_m + (1 - \phi)(\varepsilon_i + 2\varepsilon_m)}, \quad (6)$$

where

$$\tau = \frac{\phi 3\varepsilon_m + (1 - \phi)(\varepsilon_i + 2\varepsilon_m)}{\phi 3\sigma_m + (1 - \phi)(\sigma_i + 2\sigma_m)}. \quad (7)$$

### B. Effective permittivity of a ferroelectric 0-3 composite

For dielectric measurement, assume  $\langle E_3 \rangle = E_0 \sin \omega t$  where  $\omega = 2\pi f$  and  $f$  is the frequency of the applied field. We further assume that the amplitude of  $\langle E_3 \rangle$  (i.e.,  $E_0$ ) is small such that the contribution from the hysteresis behavior may be neglected. Thus,  $\partial \langle P_{3m} \rangle / \partial t = \partial \langle P_{3i} \rangle / \partial t = 0$  in Eq. (6) which becomes

$$\frac{\partial \langle E_{3i} \rangle}{\partial t} + \frac{\langle E_{3i} \rangle}{\tau} = L_E \left\{ \frac{\partial \langle E_3 \rangle}{\partial t} + \frac{\langle E_3 \rangle}{\tau_m} \right\}, \quad (8)$$

where  $\tau_m = \varepsilon_m / \sigma_m$  and

$$L_E = \frac{3\varepsilon_m}{\phi 3\varepsilon_m + (1 - \phi)(\varepsilon_i + 2\varepsilon_m)}. \quad (9)$$

Assuming  $\langle E_{3i} \rangle$  is initially zero, the solution from solving Eq. (8) is

$$\begin{aligned} \langle E_{3i} \rangle = & \left( \frac{E_0 \tau / \tau_m}{1 + \omega^2 \tau^2} \right) L_E \{ \omega(\tau - \tau_m) e^{-t/\tau} + (1 + \omega^2 \tau \tau_m) \sin \omega t \\ & - \omega(\tau - \tau_m) \cos \omega t \}. \end{aligned} \quad (10)$$

In a dielectric measurement, the electric current flowing in the composite is used to determine the permittivity value. For a composite comprising a dilute suspension of spherical particles uniformly distributed in the matrix material, the volumetric average of the total current density may be written as

$$\langle J_3 \rangle = \langle j_3 \rangle + \partial \langle D_3 \rangle / \partial t, \quad (11)$$

where

$$\begin{cases} \langle j_3 \rangle = \phi \langle j_{3i} \rangle + (1 - \phi) \langle j_{3m} \rangle \\ \langle D_3 \rangle = \phi \langle D_{3i} \rangle + (1 - \phi) \langle D_{3m} \rangle. \end{cases} \quad (12)$$

At sufficiently long time from the start of the dielectric measurement (i.e., at steady state), the term  $\exp(-t/\tau)$  in Eq. (10) may be omitted. The components of  $\langle E_{3i} \rangle$  in phase and  $90^\circ$  out of phase with the applied field are

$$\langle E_{3i} \rangle|_{\text{in phase}} = \left( \frac{E_0 \tau / \tau_m}{1 + \omega^2 \tau^2} \right) L_E \{ (1 + \omega^2 \tau \tau_m) \sin \omega t \}, \quad (13)$$

$$\langle E_{3i} \rangle|_{\text{out of phase}} = \left( \frac{E_0 \tau / \tau_m}{1 + \omega^2 \tau^2} \right) L_E \{ \omega (\tau_m - \tau) \cos \omega t \}. \quad (14)$$

In this work, we only focus on the in-phase component of the dielectric property. The permittivity is

$$\varepsilon = \frac{\partial \int \langle J_3 \rangle dt|_{\text{in phase}}}{\partial \langle E_3 \rangle}. \quad (15)$$

Substituting Eqs. (11)–(13) into Eq. (15) and making use of Eqs. (1), (2), and (5), the effective permittivity is obtained as

$$\varepsilon = \varepsilon_m + \phi \Gamma_\varepsilon L_E (\varepsilon_i - \varepsilon_m), \quad (16)$$

where

$$\Gamma_\varepsilon = \frac{\tau \{ \tau_m^{-1} + \tau_{\text{neg}}^{-1} (1 - \tau / \tau_m) \} + \omega^2 \tau^2}{1 + \omega^2 \tau^2}, \quad (17)$$

$$\tau_{\text{neg}} = \frac{\varepsilon_i - \varepsilon_m}{\sigma_i - \sigma_m}, \quad (18)$$

or in a more familiar form,

$$\varepsilon = \varepsilon_m \frac{(\varepsilon_i + 2\varepsilon_m) + (3\Gamma_\varepsilon - 1)\phi(\varepsilon_i - \varepsilon_m)}{(\varepsilon_i + 2\varepsilon_m) - \phi(\varepsilon_i - \varepsilon_m)}. \quad (19)$$

Note that when  $\sigma_i = \sigma_m = 0$ ,  $\Gamma_\varepsilon = 1$  and Eq. (19) reduces to the well-known Maxwell–Wagner formula.<sup>11</sup>

### C. Effective piezoelectric coefficients of a ferroelectric 0-3 composite

In the piezoelectric measurement, the polarizations  $\langle P_{3i} \rangle$  and  $\langle P_{3m} \rangle$  vary with the applied stress (piezoelectricity). Suppose the composite is subjected to an external tensile stress  $T$ . The rates of change of polarizations in Eq. (6) can be related to the external stress due to piezoelectric effect. Thus (see Appendix),

$$\begin{cases} \frac{\partial \langle P_{3i} \rangle}{\partial t} = \mathbf{d}_i \frac{\partial T}{\partial t} \\ \frac{\partial \langle P_{3m} \rangle}{\partial t} = \mathbf{d}_m \frac{\partial T}{\partial t}, \end{cases} \quad (20)$$

where  $\mathbf{d}_i = \partial \langle P_{3i} \rangle / \partial T$ ,  $\mathbf{d}_m = \partial \langle P_{3m} \rangle / \partial T$ . When the stress is applied along the  $x$  direction, i.e.,  $T = T_{xx}$ , then  $\mathbf{d}_i = \mathbf{d}_i^\perp$  and  $\mathbf{d}_m = \mathbf{d}_m^\perp$ , where

$$\mathbf{d}_i^\perp = (L_T^\parallel + L_T^\perp) d_{31i} + L_T^\perp d_{33i}, \quad (21)$$

$$\mathbf{d}_m^\perp = (\bar{L}_T^\parallel + \bar{L}_T^\perp) d_{31m} + \bar{L}_T^\perp d_{33m}, \quad (22)$$

and

$$L_T^\perp = \frac{I_T}{1 - \phi(1 - 3I_T)} - \frac{J_T}{1 - \phi(1 - 3J_T)}, \quad (23)$$

$$L_T^\parallel = \frac{I_T}{1 - \phi(1 - 3I_T)} + \frac{2J_T}{1 - \phi(1 - 3J_T)}, \quad (24)$$

$$\bar{L}_T^\perp = \frac{-\phi L_T^\perp}{1 - \phi} = \frac{1}{3} \left[ \frac{1}{1 - \phi(1 - 3I_T)} - \frac{1}{1 - \phi(1 - 3J_T)} \right], \quad (25)$$

$$\bar{L}_T^\parallel = \frac{1 - \phi L_T^\parallel}{1 - \phi} = \frac{1}{3} \left[ \frac{1}{1 - \phi(1 - 3I_T)} + \frac{2}{1 - \phi(1 - 3J_T)} \right], \quad (26)$$

$$I_T = \frac{1}{3} \frac{k_i}{k_m} \frac{3k_m + 4\mu_m}{3k_i + 4\mu_m}, \quad (27)$$

$$J_T = \frac{5}{3} \frac{(3k_m + 4\mu_m)\mu_i}{6(k_m + 2\mu_m)\mu_i + (9k_m + 8\mu_m)\mu_m}. \quad (28)$$

Here  $d_{31}$  and  $d_{33}$  are the piezoelectric coefficients.  $k$  and  $\mu$  denote bulk modulus and shear modulus, respectively. When the stress acts along the  $z$  direction, i.e.,  $T = T_{zz}$ , then  $\mathbf{d}_i = \mathbf{d}_i^\parallel$  and  $\mathbf{d}_m = \mathbf{d}_m^\parallel$ , where

$$\mathbf{d}_i^\parallel = L_T^\parallel d_{33i} + 2L_T^\perp d_{31i}, \quad (29)$$

$$\mathbf{d}_m^\parallel = \bar{L}_T^\parallel d_{33m} + 2\bar{L}_T^\perp d_{31m}. \quad (30)$$

In short-circuit condition (i.e.,  $\langle E_3 \rangle = 0$ ), Eq. (6) becomes

$$\frac{\partial \langle E_{3i} \rangle}{\partial t} + \frac{\langle E_{3i} \rangle}{\tau} = \frac{(1 - \phi)(\mathbf{d}_m - \mathbf{d}_i)}{\phi 3\varepsilon_m + (1 - \phi)(\varepsilon_i + 2\varepsilon_m)} \frac{\partial T}{\partial t}. \quad (31)$$

Assuming  $T = T_0 \sin \omega t$  with  $T_0$  being the amplitude of applied stress and  $\langle E_{3i} \rangle$  is initially zero, the solution from solving Eq. (31) is

$$\begin{aligned} \langle E_{3i} \rangle &= \left( \frac{T_0 \omega \tau}{1 + \omega^2 \tau^2} \right) \frac{(1 - \phi)(\mathbf{d}_m - \mathbf{d}_i)}{\phi 3\varepsilon_m + (1 - \phi)(\varepsilon_i + 2\varepsilon_m)} \\ &\quad \times (\omega \tau \sin \omega t + \cos \omega t - e^{-t/\tau}), \end{aligned} \quad (32)$$

where  $\omega = 2\pi f$  and  $f$  is the frequency of the applied stress. From Eq. (5),  $\langle E_{3m} \rangle = -\phi \langle E_{3i} \rangle / (1 - \phi)$ , since  $\langle E_3 \rangle = 0$  in the piezoelectric measurement.

For a sufficiently long time in the piezoelectric measurement (i.e., at steady state), the term  $\exp(-t/\tau)$  in Eq. (32) may be omitted. The components of  $\langle E_{3i} \rangle$  in phase and  $90^\circ$  out of phase with the applied stress are

$$\langle E_{3i} \rangle|_{\text{in phase}} = \left( \frac{T_0 \omega^2 \tau^2}{1 + \omega^2 \tau^2} \right) \frac{(1 - \phi)(\mathbf{d}_m - \mathbf{d}_i) \sin \omega t}{\phi 3 \varepsilon_m + (1 - \phi)(\varepsilon_i + 2\varepsilon_m)}, \quad (33)$$

$$\langle E_{3i} \rangle|_{\text{out of phase}} = \left( \frac{T_0 \omega \tau}{1 + \omega^2 \tau^2} \right) \frac{(1 - \phi)(\mathbf{d}_m - \mathbf{d}_i) \cos \omega t}{\phi 3 \varepsilon_m + (1 - \phi)(\varepsilon_i + 2\varepsilon_m)}. \quad (34)$$

Again, we only focus on the in-phase component of the piezoelectric responses. The piezoelectric  $d$  coefficient of the composite obtained from the measurement is

$$d = \frac{\partial \left\langle \int \langle J_3 \rangle dt \right\rangle_{\text{in phase}}}{\partial \langle T \rangle}. \quad (35)$$

Substituting Eq. (33) into Eqs. (1), (2), and (12), we obtain from Eq. (35),

$$d = \phi \mathbf{d}_i + (1 - \phi) \mathbf{d}_m + \phi(1 - \phi) \Gamma_d (L_E - \bar{L}_E) (\mathbf{d}_i - \mathbf{d}_m), \quad (36)$$

where

$$\Gamma_d = \frac{\tau / \tau_{\text{neg}} + \omega^2 \tau^2}{1 + \omega^2 \tau^2}, \quad (37)$$

$$\bar{L}_E = \frac{1 - \phi L_E}{1 - \phi} = \frac{\varepsilon_i + 2\varepsilon_m}{\phi 3 \varepsilon_m + (1 - \phi)(\varepsilon_i + 2\varepsilon_m)}. \quad (38)$$

Further, using Eqs. (21), (22), (29), and (30), the effective  $d_{31}$  and  $d_{33}$  coefficients can be reexpressed as

$$d_{31} = \phi [1 - \Gamma_d (1 - L_E)] \{ (L_T^\parallel + L_T^\perp) d_{31i} + L_T^\perp d_{33i} \} + (1 - \phi) \times [1 - \Gamma_d (1 - \bar{L}_E)] \{ (\bar{L}_T^\parallel + \bar{L}_T^\perp) d_{31m} + \bar{L}_T^\perp d_{33m} \}, \quad (39)$$

$$d_{33} = \phi [1 - \Gamma_d (1 - L_E)] \{ L_T^\parallel d_{33i} + 2L_T^\perp d_{31i} \} + (1 - \phi) \times [1 - \Gamma_d (1 - \bar{L}_E)] \{ \bar{L}_T^\parallel d_{33m} + 2\bar{L}_T^\perp d_{31m} \}. \quad (40)$$

The effective hydrostatic piezoelectric  $d_h$  coefficient is defined by  $d_h = d_{33} + 2d_{31}$  (and similarly for inclusion and matrix), thus,

$$d_h = \phi [1 - \Gamma_d (1 - L_E)] L_T^h d_{hi} + (1 - \phi) [1 - \Gamma_d (1 - \bar{L}_E)] \bar{L}_T^h d_{hm}, \quad (41)$$

where

$$L_T^h = 2L_T^\perp + L_T^\parallel = \frac{(3k_m + 4\mu_m)k_i}{(3k_m + 4\mu_m\phi)k_i + 4(1 - \phi)\mu_m k_m}, \quad (42)$$

$$\begin{aligned} \bar{L}_T^h &= 2\bar{L}_T^\perp + \bar{L}_T^\parallel \\ &= \frac{1 - \phi L_T^h}{1 - \phi} = \frac{(3k_i + 4\mu_m)k_m}{(3k_m + 4\mu_m\phi)k_i + 4(1 - \phi)\mu_m k_m}. \end{aligned} \quad (43)$$

Note that when  $\sigma_i = \sigma_m = 0$ ,  $\Gamma_d = 1$  and Eqs. (39)–(41) reduce to the expressions of our previous model.<sup>12</sup>

## D. Effective piezoelectric coefficients of a composite in terms of effective $\varepsilon$ , $k$ , and $\mu$

The foregoing Eqs. (39)–(41) are calculated for the dilute suspension regime. One can reexpress the  $L_E$ 's and  $L_T$ 's [Eqs. (9), (37), (23)–(26), (42), and (43)] in terms of the effective dielectric and elastic properties of the composite as in Ref. 12.  $L_E$  may be directly reexpressed from Eq. (16) and relabeled  $\ell_E$ ,

$$\ell_E = \frac{1}{\phi \Gamma_\varepsilon} \frac{\varepsilon - \varepsilon_m}{\varepsilon_i - \varepsilon_m}. \quad (44)$$

A similar derivation can also be made for reexpressing  $\bar{L}_E$ . Using Eqs. (1)–(5) and again assuming  $\partial \langle P_{3m} \rangle / \partial t = \partial \langle P_{3i} \rangle / \partial t = 0$ , we can write

$$\frac{\partial \langle E_{3m} \rangle}{\partial t} + \frac{\langle E_{3m} \rangle}{\tau} = \bar{L}_E \left\{ \frac{\partial \langle E \rangle}{\partial t} + \frac{\langle E \rangle}{\tau_{\text{pos}}} \right\}, \quad (45)$$

where  $\tau_{\text{pos}} = (\varepsilon_i + 2\varepsilon_m) / (\sigma_i + 2\sigma_m)$ . The solution of Eq. (45) for the same sinusoidal input is

$$\begin{aligned} \langle E_{3m} \rangle &= \left( \frac{E_0 \tau / \tau_{\text{pos}}}{1 + \omega^2 \tau^2} \right) \bar{L}_E \{ \omega(\tau - \tau_{\text{pos}}) e^{-t/\tau} \\ &\quad + (1 + \omega^2 \tau \tau_{\text{pos}}) \sin \omega t - \omega(\tau - \tau_{\text{pos}}) \cos \omega t \}. \end{aligned} \quad (46)$$

We then follow the same footsteps as before in deriving Eq. (16) and finally obtain

$$\varepsilon = \varepsilon_m - (1 - \phi) \bar{\Gamma}_\varepsilon \bar{L}_E (\varepsilon_i - \varepsilon_m), \quad (47)$$

where

$$\bar{\Gamma}_\varepsilon = \frac{\tau \{ \tau_{\text{pos}}^{-1} + \tau_{\text{neg}}^{-1} (1 - \tau / \tau_{\text{pos}}) \} + \omega^2 \tau^2}{1 + \omega^2 \tau^2} \quad (48)$$

and  $\bar{L}_E$  is as given by Eq. (38). After solving for  $\bar{L}_E$  by rearranging Eq. (47) and relabeling by  $\bar{\ell}_E$ , we obtain

$$\bar{\ell}_E = \frac{1}{(1 - \phi) \bar{\Gamma}_\varepsilon} \frac{\varepsilon_i - \varepsilon}{\varepsilon_i - \varepsilon_m}. \quad (49)$$

Concerning  $L_T$ 's, we can adopt the same transformed expressions (called  $F_T$ 's) as in Ref. 12. This technique has been demonstrated there to give results which are applicable to higher  $\phi$ , provided that better estimates of effective properties are available. This scheme provides simple and tractable explicit expressions for higher  $\phi$ . Thus Eqs. (39)–(41) are transformed to

$$d_{31} = \phi [1 - \Gamma_d (1 - \ell_E)] \{ (F_T^\parallel + F_T^\perp) d_{31i} + F_T^\perp d_{33i} \} + (1 - \phi) \times [1 - \Gamma_d (1 - \bar{\ell}_E)] \{ (\bar{F}_T^\parallel + \bar{F}_T^\perp) d_{31m} + \bar{F}_T^\perp d_{33m} \}, \quad (50)$$

$$d_{33} = \phi [1 - \Gamma_d (1 - \ell_E)] \{ F_T^\parallel d_{33i} + 2F_T^\perp d_{31i} \} + (1 - \phi) [1 - \Gamma_d (1 - \bar{\ell}_E)] \{ \bar{F}_T^\parallel d_{33m} + 2\bar{F}_T^\perp d_{31m} \}, \quad (51)$$

$$d_h = \phi[1 - \Gamma_d(1 - \ell_E)]F_T^h d_{hi} + (1 - \phi) \times [1 - \Gamma_d(1 - \bar{\ell}_E)]\bar{F}_T^h d_{hm}, \quad (52)$$

where

$$F_T^\perp = \frac{1}{\phi} \left\{ \frac{1}{3} \frac{k^{-1} - k_m^{-1}}{k_i^{-1} - k_m^{-1}} - \frac{1}{3} \frac{\mu^{-1} - \mu_m^{-1}}{\mu_i^{-1} - \mu_m^{-1}} \right\}, \quad (53)$$

$$F_T^\parallel = \frac{1}{\phi} \left\{ \frac{1}{3} \frac{k^{-1} - k_m^{-1}}{k_i^{-1} - k_m^{-1}} + \frac{2}{3} \frac{\mu^{-1} - \mu_m^{-1}}{\mu_i^{-1} - \mu_m^{-1}} \right\}, \quad (54)$$

$$\bar{F}_T^\perp = \frac{-\phi F_T^\perp}{1 - \phi} = \frac{1}{1 - \phi} \left\{ \frac{1}{3} \frac{k_i^{-1} - k^{-1}}{k_i^{-1} - k_m^{-1}} - \frac{1}{3} \frac{\mu_i^{-1} - \mu^{-1}}{\mu_i^{-1} - \mu_m^{-1}} \right\}, \quad (55)$$

$$\bar{F}_T^\parallel = \frac{1 - \phi F_T^\parallel}{1 - \phi} = \frac{1}{1 - \phi} \left\{ \frac{1}{3} \frac{k_i^{-1} - k^{-1}}{k_i^{-1} - k_m^{-1}} + \frac{2}{3} \frac{\mu_i^{-1} - \mu^{-1}}{\mu_i^{-1} - \mu_m^{-1}} \right\}, \quad (56)$$

$$F_T^h = \frac{1}{\phi} \frac{k^{-1} - k_m^{-1}}{k_i^{-1} - k_m^{-1}}, \quad (57)$$

$$\bar{F}_T^h = \frac{1 - \phi F_T^h}{1 - \phi} = \frac{1}{1 - \phi} \frac{k_i^{-1} - k^{-1}}{k_i^{-1} - k_m^{-1}}. \quad (58)$$

In the above, we have assumed that the value of  $\Gamma_d$  is unchanged.

### III. RESULTS AND DISCUSSION

A previous article<sup>5</sup> reported that the piezoelectric  $d_{33}$  coefficient and permittivity of a PZT/PVDF 0-3 composite would be significantly increased by solvent treatment. The samples were immersed in a certain solvent (e.g., DMA) for a period of time and the piezoelectric and dielectric properties were measured after the samples were removed from the solvent environment. Chen *et al.* found that the dielectric constant increased from 60 to 120 and the  $d_{33}$  constant from 27 to 130 pC/N. However, the elastic constant of the composite was not changed by the solvent treatment. This suggests that the anomaly is not directly related to the structural (configurational) changes in the treated composite which may be induced by the diffusion of solvent as the authors postulated. The phenomenon is most likely the effect of the dramatic increment of electrical conductivity. Since the conductivity of solvent combinations such as ethylene carbonate (EC), propylene carbonate (PC), dimethylacetamide (DMA), dimethylformamide (DMF), and dimethylsulphoxide (DMSO) are about  $10^{-6} \Omega^{-1} \text{cm}^{-1}$ ,<sup>9</sup> the effective conductivity of PVDF is thought to be dramatically increased, especially when the composite sample is just taken out from the solvent environment. On the other hand, Chen *et al.* also observed that, after several hours, both the anomalous dielectric and piezoelectric constants gradually decreased to their virgin values again. This is consistent with the thinking that the conductivity in the matrix phase diminishes as the solvent evaporates away.

TABLE I. Properties of constituents for PZT/PVDF 0-3 composites.

	$\varepsilon/\varepsilon_0^a$	$\sigma$ ( $\Omega^{-1} \text{cm}^{-1}$ )	$Y^a$ (GPa)	$\nu^b$	$d_{33}$ (pC/N)	$-d_{31}$ (pC/N)
PZT	1100	$5 \times 10^{-14c}$	36	0.3	330 <sup>a</sup>	140
PVDF	12	varied	2.5	0.4	0	0

<sup>a</sup>Reference 5.

<sup>b</sup>Reference 12.

<sup>c</sup>Reference 14.

#### A. Effect of $\sigma_m$ and measuring frequency on $\varepsilon$ and $d_{33}$ coefficients of 0-3 composites

Here, we will demonstrate that high  $\sigma_m$  plays a significant role in the effective  $\varepsilon$  and  $d_{33}$ . The adopted properties of constituents for the calculations are listed in Table I.  $Y$  and  $\nu$  may be transformed to  $k$  and  $\mu$  by using  $k=Y/(3-6\nu)$  and  $\mu=Y/(2+2\nu)$ . Chen *et al.* used a dc field of 10 MV/m to polarize their composite. Since the coercive field of PVDF is about 45 MV/m,<sup>15</sup> which is much larger than the poling field adopted by Chen *et al.*, the electric field acting in the matrix phase will be insufficient to give a high degree of remanent polarization after poling, hence the piezoelectric activities will also be limited. In another report for the piezoelectric properties of PZT/PVDF composites, Furukawa *et al.* reported  $d_{31}=0.3$  pC/N for PVDF, which is negligibly small.<sup>16</sup> Hence, we adopted  $d_{33m}=d_{31m}=0$  in Table I. The calculated results of  $\varepsilon$  [Eq. (19)] and  $d_{33}$  [Eq. (40)] for PZT/PVDF 0-3 composites of small volume fraction are shown in Fig. 1. The measuring frequency for dielectric constant is 1 kHz.<sup>5</sup> For comparison purpose, we assume the same measuring frequency (the highest achievable in commercial  $d_{33}$  meters) for  $d_{33}$  constant. In Fig. 1, the solid lines are based on our previous model,<sup>12</sup> which corresponds to  $\Gamma_\varepsilon=1$  in Eq. (19) and  $\Gamma_d=1$  in Eq. (40) of the present model. A typical value of conductivity for PVDF at room temperature is about  $5 \times 10^{-12} \Omega^{-1} \text{cm}^{-1}$ . The prediction based on this  $\sigma_m$  value overlaps with our previous model. Thus, the effect of electrical conductivity on the effective  $\varepsilon$  and  $d_{33}$  of untreated samples can normally be neglected at room temperature. When  $\sigma_m$  is increased, no notable increment of  $\varepsilon$  and  $d_{33}$  is observed until  $\sigma_m=10^{-8} \Omega^{-1} \text{cm}^{-1}$ . More enhancement of  $\varepsilon$  and  $d_{33}$  is observed at higher ceramic volume fraction. Further increment of  $\sigma_m$  in order of magnitude will dramatically increase the value of  $\varepsilon$  and  $d_{33}$  for a given  $\phi$ .

In Fig. 1, we demonstrate the significant effect when  $\sigma_m \geq 10^{-8} \Omega^{-1} \text{cm}^{-1}$ . It shows that both  $\varepsilon$  and  $d_{33}$  are very sensitive to a small change of  $\sigma_m$  in this region. According to Chen *et al.*, the loading of the PZT in their composite is approximately 55%.<sup>5</sup> At high ceramic concentration, the calculated values shown in Fig. 1 do not fit well with their measured values because Eqs. (19) and (40) are derived from dilute suspension considerations, although it is already observed that  $\sigma_m$  can significantly enhance  $\varepsilon$  and  $d_{33}$ . Later on, we will use Eq. (51) (higher volume fraction calculation for  $d_{33}$ ) to predict the  $d_{33}$  values of the experimental data of Chen *et al.* In most of the calculations shown in Fig. 1,  $\sigma_i$  is taken as  $5 \times 10^{-14} \Omega^{-1} \text{cm}^{-1}$ . In Fig. 1, the predictions for  $\sigma_i=\sigma_m=5 \times 10^{-8} \Omega^{-1} \text{cm}^{-1}$  are also shown. It clearly reveals that the calculated  $\varepsilon$  and  $d_{33}$  values are only slightly different

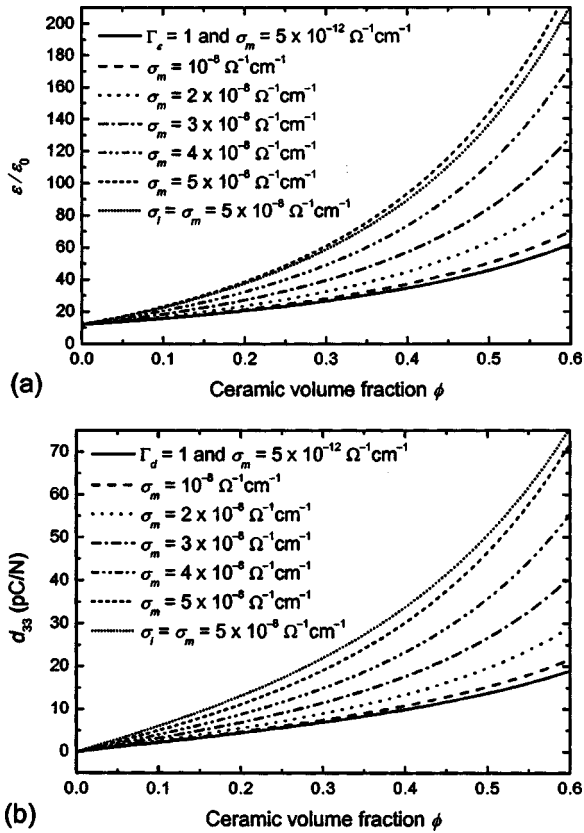


FIG. 1. The variation of (a) permittivity  $\epsilon$  [Eq. (19)] and (b)  $d_{33}$  constant [Eq. (40)] of PZT/PVDF composites with the magnitude of conductivity. Equations (19) and (40) with  $\Gamma$ 's=1 (solid lines) represent that the constituents are perfectly insulating.

from the case of  $\sigma_i = 5 \times 10^{-14} \Omega^{-1} \text{cm}^{-1}$  with the same  $\sigma_m = 5 \times 10^{-8} \Omega^{-1} \text{cm}^{-1}$ . Actually, we generally find that  $\epsilon$  and  $d_{33}$  are much less affected by  $\sigma_i$  than by  $\sigma_m$ . In addition, the enhancement of  $\epsilon$  and  $d_{33}$  shown in Fig. 1 will actually continue for increasing  $\sigma_m$  until  $\sigma_m \approx 10^{-6} \Omega^{-1} \text{cm}^{-1}$ . When  $\sigma_m > 10^{-6} \Omega^{-1} \text{cm}^{-1}$ , a steady state is reached and no further notable increment of  $\epsilon$  and  $d_{33}$  is observed. This apparent limit will be smaller for a lower measuring frequency.

In Eqs. (17) and (37),  $\tau$  is the governing factor which depends on the constituent permittivities, conductivities, and  $\phi$ , rather than just  $\sigma_i$  or  $\sigma_m$ . Moreover, one can also appreciate from Eq. (7) that the  $\sigma_i$  is of lesser significance than  $\sigma_m$ . Figure 2 shows the ceramic volume fraction dependence of  $\tau$  with different adopted  $\sigma_m$ . The figure shows that  $\tau$  decreases monotonically with  $\phi$  for all  $\sigma_m$ 's. Thus,  $\epsilon$  and  $d_{33}$  increase with ceramic volume fraction, as noted in Fig. 1. From Fig. 2, it is found that a higher  $\sigma_m$  generally displaces the whole curve to lower  $\tau$  values.

From Eqs. (17) and (37), the  $\Gamma$ 's should also be sensitive to changes in the measuring frequency. Figure 3 shows the variation of  $\epsilon$  and  $d_{33}$  with the measuring frequency  $f$ , assuming  $\sigma_m = 5 \times 10^{-12} \Omega^{-1} \text{cm}^{-1}$ . At frequencies above 1 Hz, no notable enhancement is found in  $\epsilon$  and  $d_{33}$ . Further reduction in  $f$  will have an effect similar to increasing  $\sigma_m$ , resulting in significant enhancement of  $\epsilon$  and  $d_{33}$ .

The above analyses for piezoelectricity have been confined to the  $d_{33}$  constant. Actually, the enhancement by conductivity also applies to the  $d_{31}$  [Eq. (29)] and  $d_h$  [Eq. (34)]

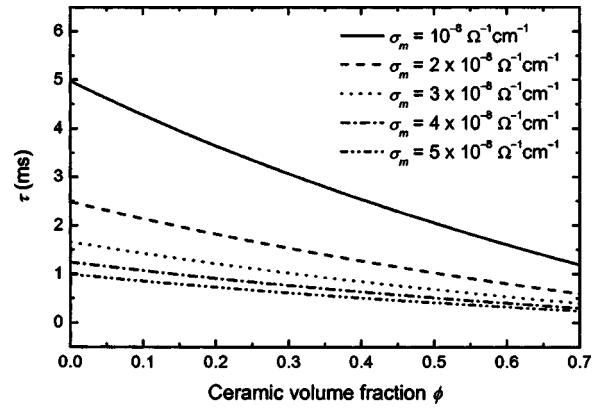


FIG. 2. The variation of  $\tau$  [Eq. (7)] of PZT/PVDF composites with the magnitude of conductivity in the matrix phase. The measuring frequency is 1 kHz.

constants. Summing up, with electrical conductivity considered, the model suggested in this article yields significant effects for composite samples with high conductivity in the polymer matrix, but only minimal effects for normal composites possessing relatively low conductivity. Thus the  $\Gamma$  factors [Eqs. (17) and (37)] do not affect in a noticeable way the goodness of fit already obtained by many existing models for ordinary composite samples. For samples possessing high  $\sigma$ , the effect of the  $\Gamma$  factors has to be included.

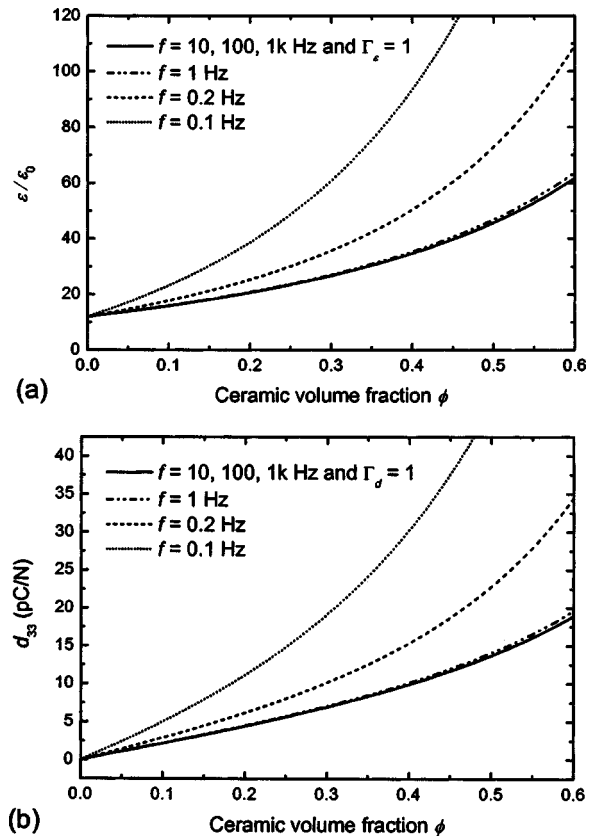


FIG. 3. The variation of (a) permittivity  $\epsilon$  [Eq. (19)] and (b)  $d_{33}$  constant [Eq. (40)] of PZT/PVDF composites with the measuring frequency. Equations (19) and (40) with  $\Gamma$ 's=1 represent that the constituents are perfectly insulating. Other lines with  $\Gamma$ 's  $\neq 1$  assumes that the constituents possess small but finite conductivity.

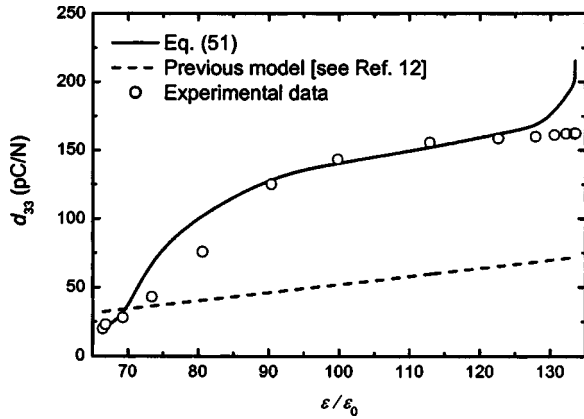


FIG. 4. Theoretical prediction by Eq. (51) is compared with the experimental data of Chen *et al.* (see Ref. 5) for the  $d_{33}$  vs  $\varepsilon$  of a PZT/PVDF composite.  $\sigma_m$  have been assumed to decay linearly with time from  $3.8 \times 10^{-8} \Omega^{-1} \text{cm}^{-1}$  to  $5 \times 10^{-12} \Omega^{-1} \text{cm}^{-1}$  and the measuring frequency is 200 Hz.

### B. Comparison with experimental data

Here we attempt to apply the present model to investigate the anomalously high  $d_{33}$  values reported by Chen *et al.*<sup>5</sup> They measured the permittivity and  $d_{33}$  constant after the PZT/PVDF samples were removed from the solvent environment and obtained very high  $\varepsilon$  and  $d_{33}$  values which decayed with time. Their experimental data demonstrated that the percentage increment of  $d_{33}$  is significantly larger than the permittivity. The variation of  $d_{33}$  with  $\varepsilon$  can be obtained from the experimental data of Chen *et al.* and is shown in Fig. 4. We can make use of Eq. (51) to predict this  $d_{33}$ - $\varepsilon$  relationship, using the experimentally measured  $\varepsilon$  and elastic constant ( $=8 \times 10^9 \text{ N m}^{-2}$ ).<sup>5</sup> In the absence of rigorous theory to model the decay of  $\sigma_m$  with time due to solvent evaporation, we assume that  $\sigma_m$  decays linearly with time. The value of  $\sigma_m$  when the sample is just removed from the solvent environment may be roughly estimated by Eq. (19). We use Eq. (19) to calculate the  $\sigma_m$ 's from the experimental  $\varepsilon$  given by Chen *et al.* and the results suggest that  $\sigma_m$  increases monotonically from  $1.5 \times 10^{-8} \Omega^{-1} \text{cm}^{-1}$  to  $3.8 \times 10^{-8} \Omega^{-1} \text{cm}^{-1}$  when  $\varepsilon$  varies from  $66\varepsilon_0$  to  $134\varepsilon_0$ . Note that the variation of  $\sigma_m$  is small which is due to the use of Eq. (19) for the dilute suspension case. In the regime of  $\varepsilon$  close to  $66\varepsilon_0$  (i.e., the sample has been removed from the solvent environment for a long time and the effect of conductivity is negligible), the calculated  $\sigma_m$  will generally be significantly larger than the true value [ $\sigma_m(\varepsilon=66\varepsilon_0)=1.5 \times 10^{-8} \Omega^{-1} \text{cm}^{-1}$  versus a typical value of  $5 \times 10^{-12} \Omega^{-1} \text{cm}^{-1}$  for untreated samples]. In the regime of  $\varepsilon$  close to  $134\varepsilon_0$  (i.e., the sample is just taken out from the solvent environment and the effect of conductivity is significant), the calculated  $\sigma_m$  by Eq. (19) may also be larger than the true value, but the discrepancy should not be as large as in the small  $\varepsilon$  regime. It is because the value of  $\sigma_m$  should be high at the large  $\varepsilon$  regime. The calculated high  $\sigma_m$  value is thought to be not so affected by a high or low  $\phi$  calculation when the effect of electrical conductivity is effectively dominating in Eq. (19). Hence,  $\sigma_m$  may be considered to have a value equal to or slightly less than  $3.8 \times 10^{-8} \Omega^{-1} \text{cm}^{-1}$  for  $\varepsilon \approx 134\varepsilon_0$  (the largest  $\varepsilon$  obtained by Chen *et al.*).

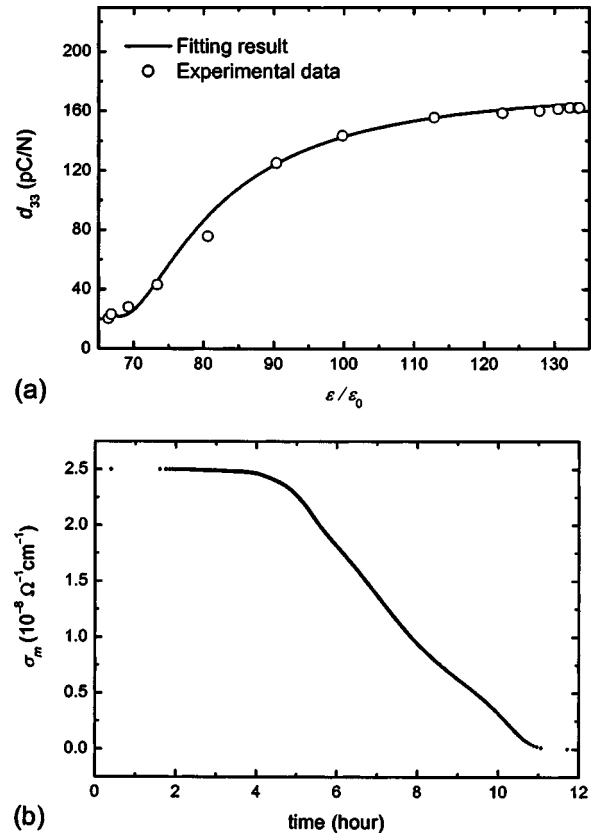


FIG. 5. (a) Mathematical fit to the experimental data of Chen *et al.* (see Ref. 5) for the  $d_{33}$  vs  $\varepsilon$  relation of a PZT/PVDF composite. (b) Calculated  $\sigma_m$  vs time using Eq. (51) shows an apparent two-stage behavior: quite constant during the first four hours and linearly decays thereafter.

Assume  $\sigma_m$  decays linearly with time from  $3.8 \times 10^{-8} \Omega^{-1} \text{cm}^{-1}$  to  $5 \times 10^{-12} \Omega^{-1} \text{cm}^{-1}$  during the 12-h measurement performed by Chen *et al.* and their  $d_{33}$  meter has a typical measuring frequency of 200 Hz. Moreover, Eq. (51) requires two elastic properties. Apart from the elastic constant measured by Chen *et al.*, we have also adopted<sup>12,17</sup>

$$k = k_m + \frac{\phi(k_i - k_m)}{1 + (1 - \phi)(k_i - k_m)/(k_m + 4\mu_m/3)} \quad (59)$$

to calculate the effective bulk modulus. Theoretical prediction of Eq. (51) with the above considerations is shown in Fig. 4. We notice that, apart from the rightmost regime of extremely large  $\varepsilon$  (when the sample is just taken out from the solvent environment), the general trend of  $d_{33}$  vs  $\varepsilon$  has been reproduced by the above simple assumption for  $\sigma_m$ . In Fig. 4, the dashed line is based on our previous model,<sup>12</sup> which corresponds to  $\Gamma_d = \Gamma_\varepsilon = \bar{\Gamma}_\varepsilon = 1$  in Eq. (51) of the present model. The prediction is very far away from the experimental data. The solid line (present model) shows a dramatic improvement. It seems that the consideration of high electrical conductivity in the matrix phase is essential to understand this interesting phenomenon.

The discrepancy in the large  $\varepsilon$  regime suggests that  $\sigma_m$  may not decay linearly at the initial time. To investigate this, we first fit the experimental data mathematically to give a smooth trend for  $d_{33}$  vs  $\varepsilon$  [see Fig. 5(a)]. Using the fitted curve, the “true” behavior of  $\sigma_m$  versus time is calculated by

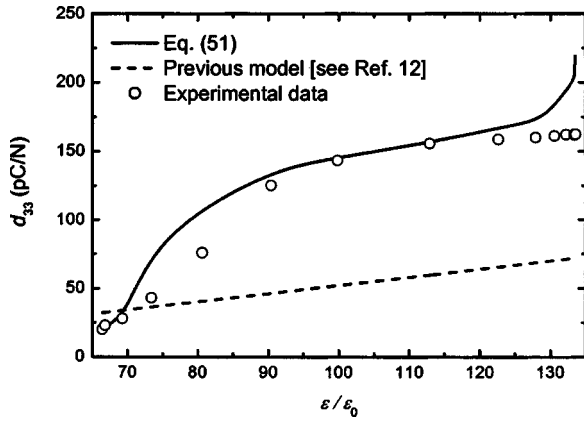


FIG. 6. Theoretical prediction by Eq. (51) is compared with the experimental data of Chen *et al.* (see Ref. 5) for the  $d_{33}$  vs  $\varepsilon$  relation of a PZT/PVDF composite.  $\sigma_m$  have been assumed to decay linearly with time from  $2 \times 10^{-8} \Omega^{-1} \text{cm}^{-1}$  to  $5 \times 10^{-12} \Omega^{-1} \text{cm}^{-1}$  and the measuring frequency is 100 Hz.

Eq. (51) and the result is shown in Fig. 5(b). The result shows an apparent two-stage  $\sigma_m$  behavior:  $\sigma_m$  changes only slowly for the first four hours, followed by a linear decay behavior similar to our assumption in the calculation of Fig. 4. This suggests that the initial evaporation of solvent, allegedly from the surface regions, may not have affected the properties in the bulk substantially because solvent diffusion from the bulk takes longer time. Further investigation is required with a more sophisticated model for solvent evaporation.

Since Chen *et al.* have not reported the measuring frequency for their piezoelectric measurement, we have assumed  $f=200$  Hz in the above analysis. If  $f=100$  Hz is adopted for our calculations, an equally good fit is obtained (solid line shown in Fig. 6). For the reduced measuring frequency, a slightly lesser  $\sigma_m$  value at  $\varepsilon=134\varepsilon_0 [=2 \times 10^{-8} \Omega^{-1} \text{cm}^{-1}]$  is adopted. This is because reducing  $f$  is effectively reducing  $\sigma_m$ , as we have demonstrated in Fig. 1.

The present formulation neglects the loss components of the elastic and piezoelectric properties in the constituents. In the case that the loss components are also considered, all constituent parameters involved should take on complex values, and the final expressions would become much more complicated.<sup>18</sup>

A variation of the present model is also suitable for the study of the pyroelectric coefficient of 0-3 composites. We may write  $\partial\langle P_{3i} \rangle / \partial t = p_i (\partial\Theta / \partial t)$  and  $\partial\langle P_{3m} \rangle / \partial t = p_m (\partial\Theta / \partial t)$  where  $p$  denotes pyroelectric coefficient and  $\Theta$  is the applied sinusoidal temperature.<sup>3</sup> The effective  $p$  can be directly rewritten from Eq. (36) as

$$p = \phi p_i + (1 - \phi) p_m + \phi(1 - \phi) \Gamma_d (L_E - \bar{L}_E) (p_i - p_m). \quad (60)$$

Thus

$$p = \phi [1 - \Gamma_d (1 - L_E)] p_i + (1 - \phi) [1 - \Gamma_d (1 - \bar{L}_E)] p_m. \quad (61)$$

This equation is a generalization of the expression suggested by Lam *et al.* who investigated the pyroelectric properties of

0-3 composites with nonpyroelectric matrix.<sup>19</sup> Note that when  $\Gamma_d=1$  (which corresponds to  $\sigma_i=\sigma_m=0$ ) and Eq. (61) reduces to the expression for primary pyroelectric coefficient suggested by Chew *et al.*<sup>20</sup>

#### IV. CONCLUSIONS

In conclusion, we have included the effect of electrical conductivity from the constituents in the prediction of dielectric and piezoelectric properties. Explicit expressions have been derived for  $\varepsilon$ ,  $d_{33}$ ,  $d_{31}$ , and  $d_h$  coefficients. High conductivity in the matrix phase can significantly enhance the permittivity and piezoelectric coefficients of ferroelectric 0-3 composites. A high  $\sigma_m$  value may be induced by solvent treatment of a composite. The enhanced  $\varepsilon$  and piezoelectric  $d$  constants have saturation values which remain unchanged beyond a certain  $\sigma_m$ . Comparison of our theoretical results with the experimental data of Chen *et al.*<sup>5</sup> shows fairly good agreement, when  $\sigma_m$  is assumed to decay roughly linearly with time due to solvent evaporation. The electrical conductivity effect is quite likely responsible for the reported anomalously high  $d_{33}$  values in the work of Chen *et al.*

#### ACKNOWLEDGMENT

This work was partially supported by the Center for Smart Materials of The Hong Kong Polytechnic University.

#### APPENDIX

Suppose the composite is subjected to tensile stresses in the  $x$ ,  $y$ , and  $z$  directions simultaneously. The contribution in polarization due to the stresses in the constituents can be written as

$$\begin{cases} \langle P_{3i} \rangle = d_{31i} \langle T_{xxi} \rangle + d_{32i} \langle T_{yyi} \rangle + d_{33i} \langle T_{zzi} \rangle \\ \langle P_{3m} \rangle = d_{31m} \langle T_{xxm} \rangle + d_{32m} \langle T_{yy m} \rangle + d_{33m} \langle T_{zzm} \rangle, \end{cases} \quad (A1)$$

where  $d_{31}$ ,  $d_{32}$ , and  $d_{33}$  are the piezoelectric coefficients and  $\langle T_{xxm} \rangle$  represents the volume-averaged stress in the  $x$  direction within the matrix material, and so forth.

In a previous article, we have considered the elasticity problem of a composite with spherical inclusions subjected to external stresses  $T_{xx}$ ,  $T_{yy}$ , and  $T_{zz}$  and obtained<sup>12</sup>

$$\begin{pmatrix} \langle T_{xxi} \rangle \\ \langle T_{yyi} \rangle \\ \langle T_{zzi} \rangle \end{pmatrix} = \begin{pmatrix} L_T^{\parallel} & L_T^{\perp} & L_T^{\perp} \\ L_T^{\perp} & L_T^{\parallel} & L_T^{\perp} \\ L_T^{\perp} & L_T^{\perp} & L_T^{\parallel} \end{pmatrix} \begin{pmatrix} T_{xx} \\ T_{yy} \\ T_{zz} \end{pmatrix}, \quad (A2)$$

$$\begin{pmatrix} \langle T_{xxm} \rangle \\ \langle T_{yy m} \rangle \\ \langle T_{zzm} \rangle \end{pmatrix} = \begin{pmatrix} \bar{L}_T^{\parallel} & \bar{L}_T^{\perp} & \bar{L}_T^{\perp} \\ \bar{L}_T^{\perp} & \bar{L}_T^{\parallel} & \bar{L}_T^{\perp} \\ \bar{L}_T^{\perp} & \bar{L}_T^{\perp} & \bar{L}_T^{\parallel} \end{pmatrix} \begin{pmatrix} T_{xx} \\ T_{yy} \\ T_{zz} \end{pmatrix}, \quad (A3)$$

where  $L_T^{\perp}$ ,  $L_T^{\parallel}$ ,  $\bar{L}_T^{\perp}$ , and  $\bar{L}_T^{\parallel}$  are given by Eqs. (11)–(14). Substituting Eqs. (A2) and (A3) into Eq. (A1) gives

$$\begin{cases} \langle P_{3i} \rangle = \{L_T^{\parallel} d_{31i} + L_T^{\perp} (d_{32i} + d_{33i})\} T_{xx} + \{L_T^{\parallel} d_{32i} + L_T^{\perp} (d_{31i} + d_{33i})\} T_{yy} + \{L_T^{\parallel} d_{33i} + L_T^{\perp} (d_{31i} + d_{32i})\} T_{zz} \\ \langle P_{3m} \rangle = \{\bar{L}_T^{\parallel} d_{31m} + \bar{L}_T^{\perp} (d_{32m} + d_{33m})\} T_{xx} + \{\bar{L}_T^{\parallel} d_{32m} + \bar{L}_T^{\perp} (d_{31m} + d_{33m})\} T_{yy} + \{\bar{L}_T^{\parallel} d_{33m} + \bar{L}_T^{\perp} (d_{31m} + d_{32m})\} T_{zz}. \end{cases} \quad (\text{A4})$$

We assume that both constituents are piezoelectrically transversely isotropic. Thus,  $d_{31i} = d_{32i}$  and  $d_{31m} = d_{32m}$  and we can write

$$\begin{cases} \frac{\partial \langle P_{3i} \rangle}{\partial t} = \mathbf{d}_i^{\perp} \frac{\partial T_{xx}}{\partial t} \\ \frac{\partial \langle P_{3m} \rangle}{\partial t} = \mathbf{d}_m^{\perp} \frac{\partial T_{xx}}{\partial t} \end{cases} \quad (\text{A5})$$

for  $T_{xx} \neq 0$  and  $T_{yy} = T_{zz} = 0$ , where  $\mathbf{d}_i^{\perp} = (L_T^{\parallel} + L_T^{\perp}) d_{31i} + L_T^{\perp} d_{33i}$  and  $\mathbf{d}_m^{\perp} = (\bar{L}_T^{\parallel} + \bar{L}_T^{\perp}) d_{31m} + \bar{L}_T^{\perp} d_{33m}$ . For  $T_{zz} \neq 0$  and  $T_{xx} = T_{yy} = 0$ ,

$$\begin{cases} \frac{\partial \langle P_{3i} \rangle}{\partial t} = \mathbf{d}_i^{\parallel} \frac{\partial T_{zz}}{\partial t} \\ \frac{\partial \langle P_{3m} \rangle}{\partial t} = \mathbf{d}_m^{\parallel} \frac{\partial T_{zz}}{\partial t}, \end{cases} \quad (\text{A6})$$

where  $\mathbf{d}_i^{\parallel} = L_T^{\parallel} d_{33i} + 2L_T^{\perp} d_{31i}$  and  $\mathbf{d}_m^{\parallel} = \bar{L}_T^{\parallel} d_{33m} + 2\bar{L}_T^{\perp} d_{31m}$ .

<sup>1</sup>W. K. Sakamoto, P. Marin-Franch, and D. K. Das-Gupta, *Sens. Actuators, A* **100**, 165 (2002).

<sup>2</sup>Y. T. Or, C. K. Wong, B. Ploss, and F. G. Shin, *J. Appl. Phys.* **93**, 4112 (2003).

<sup>3</sup>Y. T. Or, C. K. Wong, B. Ploss, and F. G. Shin, *J. Appl. Phys.* **94**, 3319

(2003).

<sup>4</sup>T. Furukawa, *IEEE Trans. Electr. Insul.* **24**, 375 (1989).

<sup>5</sup>X. D. Chen, D. B. Yang, Y. D. Jiang, Z. M. Wu, D. Li, F. J. Gou, and J. D. Yang, *Sens. Actuators, A* **65**, 194 (1998).

<sup>6</sup>G. Zukowska, M. Rogowska, A. Wojda, E. Zygadlo-Monikowska, Z. Florjańczyk, and W. Wiczorek, *Solid State Ionics* **136–137**, 1205 (2000).

<sup>7</sup>S. S. Sekhon and H. P. Singh, *Solid State Ionics* **152–153**, 169 (2002).

<sup>8</sup>A. Magistris, E. Quartarone, P. Mustarelli, Y. Saito, and H. Kataoka, *Solid State Ionics* **152–153**, 347 (2002).

<sup>9</sup>S. S. Sekhon, *Bull. Mater. Sci.* **26**, 321 (2003).

<sup>10</sup>S. S. Sekhon, N. Arora, and H. P. Singh, *Solid State Ionics* **160**, 301 (2003).

<sup>11</sup>J. C. Maxwell, *A Treatise on Electricity and Magnetism*, reprinted (Dover, New York, 1954), Vol. 1.

<sup>12</sup>C. K. Wong, Y. M. Poon, and F. G. Shin, *J. Appl. Phys.* **90**, 4690 (2001).

<sup>13</sup>C. K. Wong, Y. W. Wong, and F. G. Shin, *J. Appl. Phys.* **92**, 3974 (2002).

<sup>14</sup>H. L. W. Chan, Y. Chen, and C. L. Choy, *Integr. Ferroelectr.* **9**, 207 (1995).

<sup>15</sup>T. Ikeda, *Fundamentals of Piezoelectricity* (Oxford, New York, 1996), p. 226.

<sup>16</sup>T. Furukawa, K. Ishida, and E. Fukada, *J. Appl. Phys.* **50**, 4904 (1979).

<sup>17</sup>Z. Hashin, *J. Appl. Mech.* **29**, 143 (1962).

<sup>18</sup>C. K. Wong, Y. M. Poon, and F. G. Shin, *J. Appl. Phys.* **92**, 3287 (2002).

<sup>19</sup>K. S. Lam, Y. W. Wong, L. S. Tai, Y. M. Poon, and F. G. Shin, *J. Appl. Phys.* **96**, 3896 (2004).

<sup>20</sup>K.-H. Chew, F. G. Shin, B. Ploss, H. L. W. Chan, and C. L. Choy, *J. Appl. Phys.* **94**, 1134 (2003).